Experimental Evidence of Ca[B 12 H 12] Formation During Decomposition of a Ca(BH 4) 2 + MgH 2 Based Reactive Hydride Composite

ARTICLE *in* THE JOURNAL OF PHYSICAL CHEMISTRY C · AUGUST 2011

Impact Factor: 4.77 · DOI: 10.1021/jp204598a

12 AUTHORS, INCLUDING:

David Olid
Spanish National Research Council
8 PUBLICATIONS **131** CITATIONS
SEE PROFILE

Maria Dolors Baró
Autonomous University of Barcelona
354 PUBLICATIONS **6,345** CITATIONS
SEE PROFILE

M. Dornheim
Helmholtz-Zentrum Geesthacht
139 PUBLICATIONS **2,753** CITATIONS
SEE PROFILE

THE JOURNAL OF PHYSICAL CHEMISTRY C

ARTICLE

pubs.acs.org/JPCC

Experimental Evidence of $Ca[B_{12}H_{12}]$ Formation During Decomposition of a $Ca(BH_4)_2 + MgH_2$ Based Reactive Hydride Composite

Christian Bonatto Minella,[*,†] Sebastiano Garroni,[‡,⊥] David Olid,[§] Francesc Teixidor,[§] Claudio Pistidda,[†] Inge Lindemann,[∥] Oliver Gutfleisch,[∥] Maria Dolores Baró,[‡] Rüdiger Bormann,[†] Thomas Klassen,[†] and Martin Dornheim[†]

[†]Institute of Materials Research, Materials Technology, Helmholtz-Zentrum Geesthacht Zentrum für Material- und Küstenforschung GmbH, Max Planck Str. 1, D-21502 Geesthacht, Germany

[‡]Departament de Física, Universitat Autónoma de Barcelona, E-08193 Bellaterra, Spain

[§]Institut de Ciéncia de Materials de Barcelona, CSIC, Campus UAB, E-08193, Bellaterra, Spain

[∥]IFW Dresden, Institute for Metallic Materials, Helmholtzstrasse 20, D-01069 Dresden, Germany

Supporting Information

ABSTRACT: The combination of $Ca(BH_4)_2$ and MgH_2 materials results in a composite with remarkable hydrogen storage properties. However, full reversibility upon the (re)hydrogenation reaction has not yet been achieved. The poor reversibility is shown to be linked to the formation of stable intermediate phases or side products upon decomposition. In this work, we show, for the first time, the clear experimental evidence of $CaB_{12}H_{12}$ among the decomposition products of a $Ca(BH_4)_2 + MgH_2$ composite. A combination of ^{11}B Magic Angle Spinning−Nuclear Magnetic Resonance ($^{11}B\{^1H\}$ MAS NMR), ex situ X-ray diffraction (XRD) and Rietveld analysis are presented. An assessment of the (de)hydrogenation and (re)hydrogenation reactions of $Ca(BH_4)_2 + MgH_2$ composite is reported. The experimental results provided in this work highlight the reasons for the limited reversibility observed in the $Ca(BH_4)_2 + MgH_2$ composite upon (re)hydrogenation.

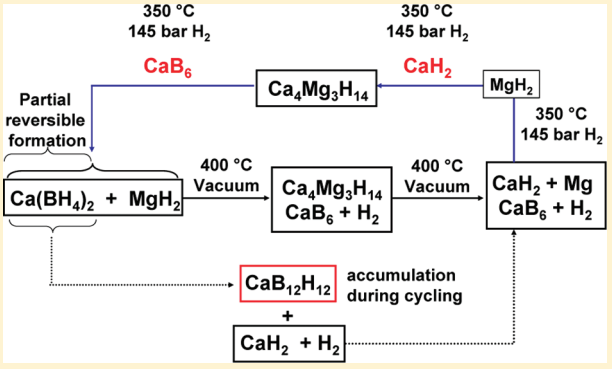

INTRODUCTION

Hydrogen is considered a promising future energy carrier due to its high abundance and its weight. In addition, its chemical energy per mass is the highest among all the chemical fuels. Solid state hydrogen storage is advantageous concerning safety and suitability compared to the liquid and compressed gas technology.[1]

Alkaline and alkaline earth metal tetrahydroborates offer high gravimetric and volumetric hydrogen densities which are among the key requirements set by the DOE (U.S. Department of Energy).[2] In the class of the promising materials for solid state hydrogen storage, $Ca(BH_4)_2$ represents an ideal candidate, due to its high gravimetric (11.5 wt %) and volumetric (~130 kg m^{-3}) hydrogen content.[3] Unfortunately, so far, most tetrahydroborates show rather sluggish kinetics and poor reversibility. The slow kinetics is linked to the high energy barrier that needs to be overcome to break or (re)form the strong B−H bond within the $[BH_4]^-$ anion. The poor reversibility is correlated to the formation of stable intermediate phases or side products during decomposition whose existence has already been predicted or reported in several works.[4−11]

Barkhordarian et al.[12] as well as Vajo et al.[13] showed that when a metal hydride (metal = Na, Li, Ca) reacts together with MgB_2, instead of boron, during the synthesis of tetrahydroborates (e.g., $Ca(BH_4)_2$, $NaBH_4$ and $LiBH_4$), the kinetic barrier is drastically reduced and full transformation can be achieved. The kinetic enhancement is linked to the peculiar layer structure of MgB_2.[12] However, upon desorption of $Ca(BH_4)_2 + MgH_2$, MgB_2 is not necessarily formed.[14] Kim et al.[15] reported CaH_2, Mg and CaB_6 to be the decomposition products. The (re)absorption reaction, at 90 bar H_2 and 350 °C for 24 h, led to the formation of $Ca(BH_4)_2 + MgH_2$ (yield of 60%) thus evidencing the important role of CaB_6 for reversibility.[15] Barkhordarian et al.[14] estimated a standard enthalpy value of 27.5 kJ mol^{-1} H_2 for the reaction involving MgB_2 and CaH_2 as decomposition products (reaction 1). No details concerning temperature and pressure values are reported. By DFT (Density Functional Theory) method, Kim et al.[15] calculated it to be 46.9 kJ mol^{-1} H_2. DFT calculations

Received: May 17, 2011
Revised: July 7, 2011
Published: August 02, 2011

for the decomposition reaction leading to CaH_2, CaB_6, and Mg (reaction 2), indicate a reaction enthalpy value of 45 kJ mol^{-1} H_2.[15] If boron is formed instead of CaB_6 (reaction 3), then the calculated reaction enthalpy value is 57.9 kJ mol^{-1} H_2.[15] The enthalpy values at 46.9, 45, and 57.9 kJ mol^{-1} H_2 are calculated at 25 °C and 1 bar H_2 pressure The decomposition paths involving formation of MgB_2 and CaB_6 upon hydrogen desorption should be the thermodynamically most favorable because the borides are exothermically formed.

$$Ca(BH_4)_2 + MgH_2 \leftrightarrow CaH_2 + MgB_2 + 4H_2 \quad (1)$$

$$Ca(BH_4)_2 + MgH_2 \leftrightarrow 2/3CaH_2 + 1/3CaB_6 + Mg + 13/3H_2 \quad (2)$$

$$Ca(BH_4)_2 + MgH_2 \leftrightarrow CaH_2 + 2B + Mg + 3H_2 \quad (3)$$

In addition, for $Ca(BH_4)_2$ itself, the following decomposition paths are possible and reported in literature:

$$Ca(BH_4)_2 \leftrightarrow 2/3CaH_2 + 1/3CaB_6 + 10/3H_2 \quad (4)$$

$$Ca(BH_4)_2 \leftrightarrow CaH_2 + 2B + 3H_2 \quad (5)$$

$$Ca(BH_4)_2 \leftrightarrow CaB_2H_2 + 3H_2 \quad (6)$$

$$Ca(BH_4)_2 \leftrightarrow CaB_2H_6 + H_2 \quad (7)$$

$$Ca(BH_4)_2 \leftrightarrow 1/6CaB_{12}H_{12} + 5/6CaH_2 + 13/6H_2 \quad (8)$$

Besides CaH_2 and H_2, different boron compounds are reported in literature: CaB_6, B (boron), CaB_2H_2, CaB_2H_6, and $CaB_{12}H_{12}$.[4,6,8,10] The calculated enthalpies of reaction are 37.04[10], 57.3[15], 31.09, and 39.2[4] or 31.34[10] kJ mol^{-1} H_2 for reactions 4, 5, 7 and 8 respectively. These values are calculated at 300 K and 1 bar H_2 pressure. For reaction 6, Zhang et al.[10] reports a reaction enthalpy value of 68.51 kJ mol^{-1} H_2, calculated at 0 K ignoring the zero-point energy.

The formation of species containing $[B_{12}H_{12}]^{2-}$ was predicted to be likely during decomposition of tetrahydroborates and their chemical stability is known to be rather high.[16] However, their detection is difficult. The existence of several amorphous polymorphs of $CaB_{12}H_{12}$ during (de)hydrogenation reaction of $Ca(BH_4)_2$ was predicted by Wang et al.[8] These phases have competing enthalpies of reaction (ΔH^{0K} = 35.8 − 37.9 kJ $mol^{-1}H_2$).[8]

Recently, Riktor et al.[6] and Lee et al.[11] observed the formation of CaB_2H_x (x = 2) (reaction 6) and of CaB_mH_n phase, respectively. Zhang et al.[10] found the phase proposed by Riktor et al.[6] too unstable to be a decomposition product. DFT and PEGS (Prototype Electrostatic Ground-State) calculations performed by Zhang et al.[10] showed CaB_2H_6 to be more likely (reaction 7). The decomposition enthalpy value of CaB_2H_6 competes in energy with that of $CaB_{12}H_{12}$ within 1 kJ mol^{-1}.[10] However, this value is over the limit of accuracy of the DFT method itself.

In the aforementioned works, X-ray diffraction was mainly employed to detect the existence of intermediate phases but, because some of them might be in the amorphous state, diffraction does not always represent the proper tool. Since $^{11}B\{^1H\}$ Solid State Magic Angle Spinning—Nuclear Magnetic Resonance (MAS NMR) does not suffer this limitation, it will be used in this work.

To the best of our knowledge, this is the first time that the clear experimental evidence of $CaB_{12}H_{12}$ in the decomposition products of $Ca(BH_4)_2$ + MgH_2 composite is reported. $CaB_{12}H_{12}$ was synthesized by chemical method and measured by $^{11}B\{^1H\}$ MAS NMR. In order to investigate the influence of such stable intermediate phases upon cycling, $^{11}B\{^1H\}$ MAS NMR analysis on the desorbed materials, up to the third hydrogen desorption, is also reported in this work.

EXPERIMENTAL SECTION

$Ca(BH_4)_2$ powder was purchased by Sigma-Aldrich. The powder consists of a mixture of low temperature γ (orthorhombic) and high temperature β-$Ca(BH_4)_2$ (tetragonal) polymorphs. MgH_2, purchased by Goldschmidt (purity 95%), was premilled in a stainless steel vial in argon atmosphere for 5 h using a Spex Mixer Mill (model 8000) and 10:1 as ball to powder ratio. One gram of powders, composed by commercial $Ca(BH_4)_2$ and premilled MgH_2, were milled together for 5 h using a Spex Mixer mill (model 8000). The milling was performed in a stainless steel vial under argon atmosphere with 10:1 as ball to powder ratio (3 spheres of 3.5 g each one and 1 g of powder). All powder handling and milling was performed in an MBraun argon box with H_2O and O_2 levels below 10 ppm to prevent contamination.

Sorption properties and kinetics were evaluated by volumetric measurements using a Sievert apparatus designed by Hydro Quebec/HERA Hydrogen Storage System. The milled powders were desorbed by heating from room temperature (25 °C) to 400 °C in static vacuum (2 kPa the starting pressure value) and afterward reabsorbed at 350 °C and 145 bar H_2 for 24 and 43 h, respectively.

Transmission X-ray diffraction measurements were performed in 0.7 mm capillaries on a Stoe Stadi P (Mo $K\alpha_1$) in Debye—Scherrer geometry. The diffractometer is equipped with a curved Ge (111) monochromator and a 6° linear position sensitive detector with a resolution of about 0.06° 2θ at full width-half-maximum (fwhm).

The MAUD software was used for the evaluation of abundance of phases by XRD patterns using Rietveld method.[17]

The calcium salt of dodecahydrododecaborate dianion was prepared from the corresponding sodium salt. It was synthesized with minor modifications of the procedure already reported in literature.[18] In order to exchange the sodium by calcium cation, an aqueous solution of the sodium salt was passed three times over a cation exchange column (cation exchange resin strongly acidic, minimum 2.0 meq/mL), charged with a 3 M solution of $CaCl_2$. The produced solution was evaporated and dried in vacuum overnight.

Solid state Magic Angle Spinning (MAS) Nuclear Magnetic Resonance (NMR) spectra were obtained using a Bruker Avance 400 MHz spectrometer with a wide bore 9.4 T magnet and employing a boron-free Bruker 4 mm CPMAS probe. The spectral frequency was 128.33 MHz for the ^{11}B nucleus and the NMR shifts are reported in parts per million (ppm) externally referenced to BF_3Et_2O. The powder materials were packed into 4 mm ZrO_2 rotors in an argon-filled glovebox and were sealed with tight fitting Kel-F caps. The one-dimensional (1D) $^{11}B\{^1H\}$ MAS NMR spectra were acquired after a 2.7 μs single $\pi/2$ pulse (corresponding to a radiofield strength of 92.6 kHz) and with application of a strong ^1H signal decoupling by using the two-pulse phase modulation (TPPM) scheme. The spectra were recorded at a MAS spinning rate of 12 kHz. Sample spinning was performed using

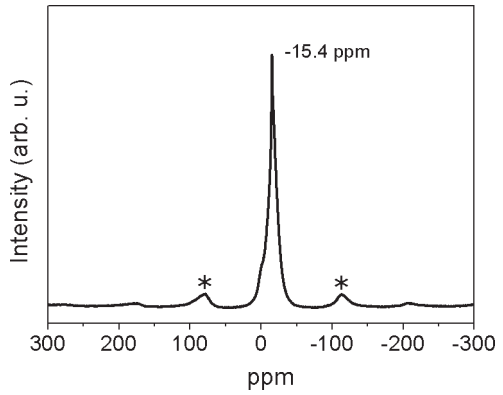

Figure 1. $^{11}B\{^1H\}$ MAS NMR spectrum at room temperature of $CaB_{12}H_{12}$. Side bands are indicated by the bold asterisks.

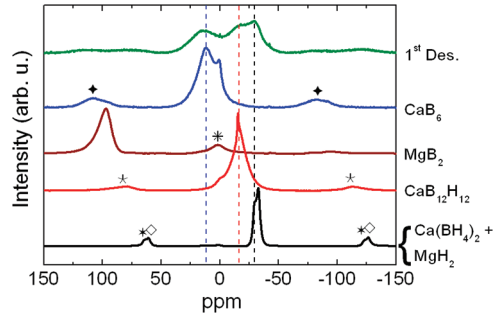

Figure 2. $^{11}B\{^1H\}$ MAS NMR spectra measured at room temperature of $Ca(BH_4)_2 + MgH_2$ composite after first desorption at 400 °C in vacuum (1st Des.) and reference compounds. Side bands are indicated by bold asterisk, open diamond, star, asterisk, and bold diamond.

dry nitrogen gas.The recovery delay was set to 10 s. Spectra were acquired at 20 °C (controlled by a BRUKER BCU unit).

RESULTS AND DISCUSSION

The $^{11}B\{^1H\}$ MAS NMR spectrum for the as-synthesized $CaB_{12}H_{12}$ is reported in Figure 1. A strong signal at −15.4 ppm is visible. This value agrees well with the chemical shift already reported in literature for $[B_{12}H_{12}]^{2-}$ species (−15.6 ppm).[7,19] The shape of the peak evidences a certain crystalline status of the as synthesized $CaB_{12}H_{12}$.

The $^{11}B\{^1H\}$ MAS NMR spectrum for the milled $Ca(BH_4)_2 + MgH_2$ after first hydrogen desorption is reported in Figure 2 together with the spectra of selected reference compounds. Milled $Ca(BH_4)_2 + MgH_2$ exhibits two signals: at −30 ppm, corresponding to the high temperature polymorph β-$Ca(BH_4)_2$ (tetragonal)[20] and at −32 ppm, belonging to the low temperature polymorph γ-$Ca(BH_4)_2$ (orthorhombic).[20] The different intensities of the peaks are linked to the abundance in the phase mixture. MgB_2 shows a very pronounced peak around 100 ppm.[7,21] The CaB_6 spectrum exhibits two lines, at +12 and +0.75 ppm, because of the two different boron sites in its structure.[22]

Three broad signals are visible in the spectrum of the desorbed material: +16, −15.6, and −30 ppm. The peak at +16 and at −30 ppm corresponds to CaB_6 and to residual β-$Ca(BH_4)_2$ respectively. The signal at −15.6 ppm belongs to $CaB_{12}H_{12}$. The same value (−15.6 ppm) was reported in literature by Hwang et al.[7] for $K_2B_{12}H_{12}$ dissolved in water. Furthermore, the aforementioned

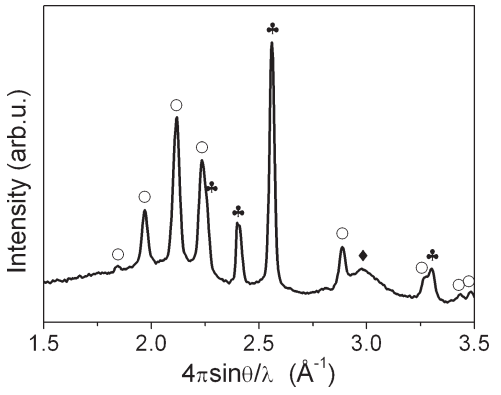

Figure 3. XRD pattern of desorbed $Ca(BH_4)_2 + MgH_2$ composite after hydrogen desorption at 400 °C in vacuum. CaH_2 (open circle); Mg (solid club); MgO (solid diamond).

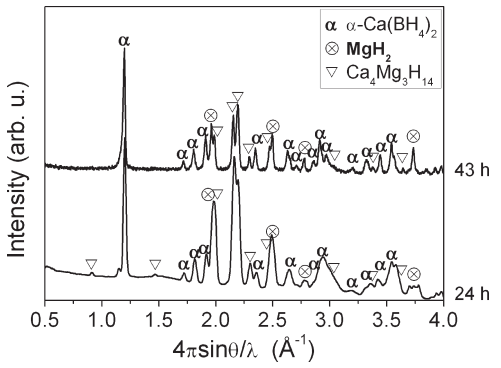

Figure 4. XRD spectra of (re)hydrogenated powders at 350 °C and 145 bar H_2 for 24 and 43 h.

three signals, for desorbed $Ca(BH_4)_2$ with NbF_5 and TiF_4 additives, were recently presented.[23]

There is a slight difference in the chemical shift of the $CaB_{12}H_{12}$ reported in Figures 1 (−15.4 ppm) and 2 (1st Des. spectrum; −15.6 ppm). The values correspond to the $CaB_{12}H_{12}$ after chemical synthesis and after desorption of $Ca(BH_4)_2 + MgH_2$ composite, respectively. Due to the broader peak in the desorbed sample, the estimation of the chemical shift value was not straightforward. A fitting of the NMR signal (not reported here) was necessary in order to evaluate the exact value (−15.6 ppm). The peak could broaden due to the disordered nature of the phase structure.[7] Such structural disorder, for the desorbed material, would contribute to explain why $CaB_{12}H_{12}$ cannot be detected by X-rays.

The presence of both CaB_6 and $CaB_{12}H_{12}$ signals, in the $^{11}B\{^1H\}$ NMR spectra of the desorbed material (Figure 2), indicates that $Ca(BH_4)_2$ simultaneously follows two decomposition paths (reactions 4 and 8). This is not surprising because of the rather similar reaction enthalpy values for the reactions leading to CaB_6 (37.04 kJ mol^{-1} H_2)[10] and $CaB_{12}H_{12}$ (39.2 or 31.34 kJ mol^{-1} H_2)[10], respectively. Although the decomposition path involving the exothermic formation of MgB_2 (reaction 1) might represent a favorable process, no significant traces are found among the final products. This is comparable to the $LiBH_4/MgH_2$ system where, under absence of hydrogen pressure, no MgB_2 is formed at temperatures below 450 °C as well.[24] Its detection should be unambiguous because its chemical shift (∼100 ppm) lies in a range completely free of other signals.

dx.doi.org/10.1021/jp204598a |J. Phys. Chem. C 2011, 115, 18010–18014

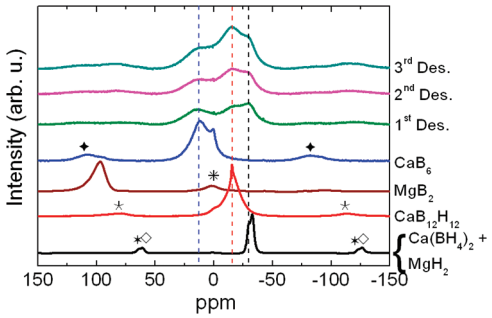

Figure 5. $^{11}B\{^1H\}$ MAS NMR spectra at room temperature of $Ca(BH_4)_2 + MgH_2$ composite after first (1st Des.), second (2nd Des.) and third (3rd Des.) hydrogen desorption at 400 °C in vacuum. Side bands are indicated by bold asterisk, open diamond, star, asterisk, and bold diamond.

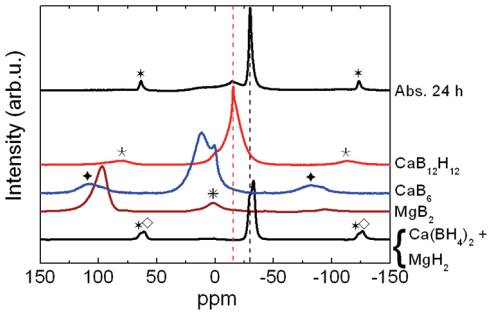

Figure 6. $^{11}B\{^1H\}$ MAS NMR spectra at room temperature of $Ca(BH_4)_2 + MgH_2$ composite after first hydrogen (re)absorption at 350 °C and 145 bar H_2 for 24 h (Abs. Twenty-four h). Side bands are indicated by bold asterisk, open diamond, asterisk, bold diamond, star, and asterisk.

Instead, as shown in Figure 3, pure Mg is present among the final compounds. The XRD pattern also exhibits reflections of CaH_2 and MgO (side product) phase. Even though the samples were handled in inert atmosphere, formation of MgO could not be avoided. This might be due to a leak present in the capillary used for the experiment.

When the desorbed materials (CaH_2, CaB_6, Mg, and $CaB_{12}H_{12}$) are (re)absorbed at 350 °C and 145 bar H_2 for 24 or 43 h, partial reversible formation of $Ca(BH_4)_2$ is achieved. The XRD spectra are shown in Figure 4.

As the result of the (re)hydrogenation reaction, MgH_2 and $Ca_4Mg_3H_{14}$[25] are formed. The latter is the product of the reaction between CaH_2 and MgH_2. After (re)hydrogenation, $Ca(BH_4)_2$ exists as α polymorph, another low temperature modification.[20] $CaB_{12}H_{12}$ does not participate in any reaction due to its stability at these experimental conditions.[26] The relative abundance after 24 h reaction, calculated by Rietveld method, is 43 (±5% error), 27 (±5% error), and 30 wt % (±5% error) for α-$Ca(BH_4)_2$, MgH_2 and $Ca_4Mg_3H_{14}$, respectively. After 43 h, they convert to 63 (±5% error), 26 (±5% error) and 11 wt % (±5% error). These values, for $Ca(BH_4)_2$, would lead to a final reversibility of 52 and 76%, after 24 and 43 h respectively. Unfortunately, these quantities are overestimated since they do not take into account the amount of amorphous or nanocrystalline $CaB_{12}H_{12}$.

In order to understand how the $Ca(BH_4)_2 + MgH_2$ composite is reversibly formed during absorption, it is important to focus on the aforementioned relative abundances. Even though the reaction time is extended (from 24 to 43 h), MgH_2 maintains a constant value (from 26 to 27 wt %). While $Ca_4Mg_3H_{14}$ is consumed (from 30 to 11 wt %), $Ca(BH_4)_2$ increases its content (from 43 to 63 wt %). This can only be explained by the reaction between $Ca_4Mg_3H_{14}$ and CaB_6 to form $Ca(BH_4)_2 + MgH_2$, as already reported in literature.[27] Upon hydrogen absorption, the Mg combines with H_2 to form MgH_2 which quickly reacts with CaH_2 to produce $Ca_4Mg_3H_{14}$. As inferred by the variation of the values of the relative abundance, $Ca_4Mg_3H_{14}$ combines with CaB_6 to form $Ca(BH_4)_2 + MgH_2$. Therefore, our findings are consistent with the hydrogenation mechanism proposed by Kim et al.[27]

With the purpose of better understanding the role of $CaB_{12}H_{12}$ during cycling of the material and whether it limits the reversible formation of $Ca(BH_4)_2$, $^{11}B\{^1H\}$ MAS NMR analysis were performed on samples after first, second, and third hydrogen desorption. The spectra are reported in Figure 5.

The same $^{11}B\{^1H\}$ MAS NMR spectra are observed for all the desorbed materials. All of them show three signals at +16, −15.6, and −30 ppm belonging to CaB_6, $CaB_{12}H_{12}$, and residual β-$Ca(BH_4)_2$, respectively. XRD analysis reveals that pure Mg and CaH_2 are also present among the final products. These results imply that, under these experimental conditions, $Ca(BH_4)_2$ always follows the same two decomposition paths leading to the formation of CaB_6 and $CaB_{12}H_{12}$. Figure 5 highlights the increase of the relative intensity of the $CaB_{12}H_{12}$ signal and therefore its quantity, during cycling compared to both signals of CaB_6 and residual β-$Ca(BH_4)_2$. This experimental evidence explains why $Ca(BH_4)_2$ suffers limited reversibility. Once $CaB_{12}H_{12}$ is formed upon desorption, due to its high stability,[8,10] it does not participate in the reversible reaction to form $Ca(BH_4)_2$. $^{11}B\{^1H\}$ MAS NMR analysis, on the (re)absorbed powder (at 145 bar H_2 and 350 °C for 24 h) is reported in Figure 6. Besides the peak of α-$Ca(BH_4)_2$, the analysis still evidence the $CaB_{12}H_{12}$ signal contributing to explain its reluctance to react. Therefore, during desorption, the $Ca(BH_4)_2 + MgH_2$ composite decomposes into $CaB_{12}H_{12}$, CaH_2, CaB_6, Mg, and H_2. Note that $CaB_{12}H_{12}$ is only formed during desorption. Of course, under the experimental conditions reported in this work, the reversible formation will always be partial due to the stable presence of $CaB_{12}H_{12}$.

CONCLUSIONS

This work reports, for the first time, on the experimental confirmation of $CaB_{12}H_{12}$ among the decomposition products of $Ca(BH_4)_2 + MgH_2$ composite. Evidence of the two simultaneous decomposition paths for $Ca(BH_4)_2$ (leading to both $CaB_{12}H_{12}$ and CaB_6) upon (de)hydrogenation reaction, is showed. An assessment of the role of $CaB_{12}H_{12}$ during cycling and its counteractive effect during (re)hydrogenation reaction is performed. The hydrogen absorption mechanism observed in this work is consistent with the literature.

ASSOCIATED CONTENT

Supporting Information. This material is available free of charge via the Internet at http://pubs.acs.org.

AUTHOR INFORMATION

Corresponding Author

*Phone: +49-(0)-4152-87-2689; Fax: +49-(0)-4152-87-2625; E-mail: christian.bonatto@hzg.de .

Present Addresses
[⊥]Dipartimento di Chimica, Università di Sassari and INSTM, Via Vienna 2, I-07100 Sassari, Italy

■ ACKNOWLEDGMENT

The authors are grateful to Marie-Curie European Research Training Network (Contract MRTN-CT-2006-035366/COSY) for the financial support. We thank the Servei de Resonància Magnètica Nuclear RMN at UAB for their technical assistance. S. G. thanks P. Nolis for useful discussions. The author M.D.B. was partially supported by ICREA ACADEMIA award. The authors F.T. and D.O. thank Generalitat de Catalunya 2009/SGR/279 and Spanish Ministry of Education CTQ2010-16237 for financial support. D.O. is enrolled in the PhD program of the UAB. D.O. thanks the Spanish Ministry of Education for an FPU grant. The authors (I.L. and O.G.) thank the European Union as well as the Free State of Saxony (ECEMP 13853/2379).

■ REFERENCES

(1) Dornheim, M. *Tailoring Reaction Enthalpies of Hydrides*; Chapter in Handbook of Hydrogen Storage; edited by Hirscher, M., Wiley-VCH; New York 2010.
(2) http://www1.eere.energy.gov/hydrogenandfuelcells/storage/index.html
(3) Buchter, F.; Łodziana, Z.; Remhof, A.; Friedrichs, O.; Borgschulte, A.; Mauron, Ph.; Züttel, A.; Sheptyakov, D.; Barkhordarian, G.; Bormann, R.; et al. *J. Phys. Chem. B* **2008**, *112*, 8042–8048.
(4) Ozolins, V.; Majzoub, E. H.; Wolverton, C. *J. Am. Chem. Soc.* **2009**, *131*, 230–237.
(5) Riktor, M. D.; Sørby, M. H.; Chłopek, K.; Fichtner, M.; Buchter, F.; Züttel, A.; Hauback, B. C. *J. Mater. Chem.* **2007**, *17*, 4939–4942.
(6) Riktor, M. D.; Sørby, M. H.; Chłopek, K.; Fichtner, M.; Hauback, B. C. *J. Mater. Chem.* **2009**, *19*, 2754–2759.
(7) Hwang, S.-J.; Bowman, R. C., Jr.; Reiter, J. W.; Rijssenbeek, J.; Soloveichik, G. L.; Zhao, J.-C.; Kabbour, H.; Ahn, C. C. *J. Phys. Chem. C* **2008**, *112*, 3164–3169.
(8) Wang, L.-L.; Graham, D. D.; Robertson, I. M.; Johnson, D. D. *J. Phys. Chem. C* **2009**, *113*, 20088–20096.
(9) Caputo, R.; Garroni, S.; Olid, D.; Teixidor, F.; Suriñach, S.; Baró, M. D. *Phys. Chem. Chem. Phys.* **2010**, *12*, 15093–15100.
(10) Zhang, Y.; Majzoub, E.; Ozolins, V.; Wolverton, C. *Phys. Rev. B* **2010**, *82*, 174107.
(11) Lee, J. Y.; Ravnsbæk, D.; Lee, Y.-S.; Kim, Y.; Cerenius, Y.; Shim, J.-H.; Jensen, T. R.; Hur, N. H.; Cho, Y. W. *J. Phys. Chem. C* **2009**, *113*, 15080–15086.
(12) Barkhordarian, G.; Klassen, T.; Dornheim, M.; Bormann, R. *J. Alloys Compd.* **2007**, *440*, L18–L21.
(13) Vajo, J. J.; Olson, G. L. *Scr. Mater.* **2007**, *56*, 829–834.
(14) Barkhordarian, G.; Jensen, T. R.; Doppiu, S.; Bösenberg, U.; Borgschulte, A.; Gremaud, R.; Cerenius, Y.; Dornheim, M.; Klassen, T.; Bormann, R. *J. Phys. Chem. C* **2008**, *112*, 2743–2749.
(15) Kim, Y.; Reed, D.; Lee, Y.-S.; Lee, J. Y.; Shim, J.-H.; Book, D.; Cho, Y. W. *J. Phys. Chem. C* **2009**, *113*, 5865–5871.
(16) Sivaev, I. B.; Sjoberg, S.; Bregadze, V. I.; Gabel, D. *Tetrahedron Lett.* **1999**, *40*, 3451–3454.
(17) Lutterotti, L.; Matthies, S.; Wenk, H.-R.; Schultz, A. J.; Richardson, J. *J. Appl. Phys.* **1997**, *81* (2), 594–600.
(18) Geis, V.; Guttsche, K.; Knapp, C; Scherer, H.; Uzun, R. *Dalton Trans.* **2009**, *15*, 2687–2694.
(19) Hermanek, S. *Chem. Rev.* **1992**, *92* (2), 325–362.
(20) Filinchuk, Y.; Rönnebro, E.; Chandra, D. *Acta Mater.* **2009**, *57*, 732–738.
(21) Pistidda, C.; Garroni, S.; Dolci, F.; Gil Bardaji, E.; Khandelwal, A.; Nolis, P.; Dornheim, M.; Gosalawit, R.; Jensen, T. R.; Cerenius, Y.; et al. *J. Alloys Compd.* **2010**, *508* (1), 212–215.
(22) Mean, B. J.; Lee, K. H.; Kang, K. H.; Lee, M.; Rhee, J. S.; Cho, B. K. *Physica B* **2005**, *359−361*, 1204–1206.
(23) Bonatto Minella, C.; Garroni, S.; Pistidda, C.; Gosalawit-Utke, R.; Barkhordarian, G.; Rongeat, C.; Lindemann, I.; Gutfleisch, O.; Jensen, T. R.; Cerenius, Y.; et al. *J. Phys. Chem. C* **2011**, *115*, 2497–2504.
(24) Bösenberg, U.; Ravnsbaek, D.; Hagemann, H.; ĎAnna, V.; Bonatto Minella, C.; Pistidda, C.; van Beek, W.; Jensen, T. R.; Bormann, R.; Dornheim, M. *J. Phys. Chem. C* **2010**, *114*, 15212–15217.
(25) Gingl, F.; Bonhomme, F.; Yvon, K.; Fischer, P. *J. Alloys Compd.* **1992**, *185*, 273–278.
(26) Stavila, V.; Her, J.-H.; Zhou, W.; Hwang, S.-J.; Kim, C.; Ottley, L. A. M.; Udovic, T. *J. Solid State Chem.* **2010**, *183*, 1133–1140.
(27) Kim, Y.; Reed, D.; Lee, Y.-S.; Shim, J.-H.; Han, H. N.; Book, D.; Cho, Y. W. *J. Alloys Compd.* **2010**, *492*, 597–600.